

See discussions, stats, and author profiles for this publication at: <https://www.researchgate.net/publication/258921356>

# Isotopic Ratio Outlier Analysis Global Metabolomics of *Caenorhabditis elegans*

ARTICLE *in* ANALYTICAL CHEMISTRY · NOVEMBER 2013

Impact Factor: 5.64 · DOI: 10.1021/ac4025413 · Source: PubMed

---

CITATIONS

12

READS

32

9 AUTHORS, INCLUDING:



Timothy J Garrett

University of Florida

50 PUBLICATIONS 769 CITATIONS

[SEE PROFILE](#)



Robert F Menger

University of Florida

6 PUBLICATIONS 49 CITATIONS

[SEE PROFILE](#)



Richard A Yost

University of Florida

174 PUBLICATIONS 4,477 CITATIONS

[SEE PROFILE](#)



Chris Beecher

NextGen Metabolomics

79 PUBLICATIONS 5,281 CITATIONS

[SEE PROFILE](#)

# Isotopic Ratio Outlier Analysis Global Metabolomics of *Caenorhabditis elegans*

Gregory S. Stupp,<sup>†,●</sup> Chaevien S. Clendinen,<sup>†,●</sup> Ramadan Ajredini,<sup>†,●</sup> Mark A. Szewc,<sup>‡</sup> Timothy Garrett,<sup>§,⊥</sup> Robert F. Menger,<sup>||</sup> Richard A. Yost,<sup>⊥,||</sup> Chris Beecher,<sup>◆</sup> and Arthur S. Edison\*,<sup>†,⊥</sup>

<sup>†</sup>Department of Biochemistry and Molecular Biology, University of Florida, Gainesville, FL

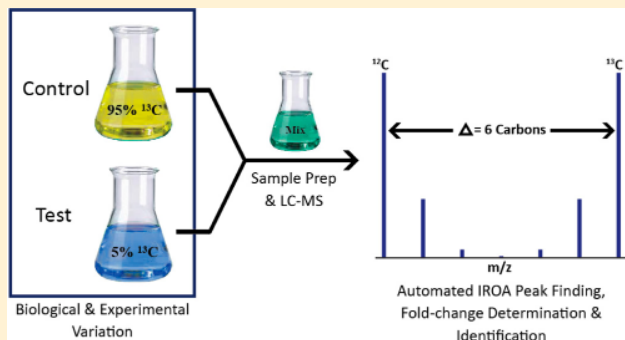
<sup>‡</sup>Thermo Fisher Scientific, Somerset, NJ

<sup>§</sup>Department of Pathology, Immunology, and Laboratory Medicine, <sup>⊥</sup>Southeast Center for Integrated Metabolomics, <sup>||</sup>Department of Chemistry, University of Florida, Gainesville, FL

<sup>◆</sup>IROA Technologies, Ann Arbor, MI

## Supporting Information

**ABSTRACT:** We demonstrate the global metabolic analysis of *Caenorhabditis elegans* stress responses using a mass-spectrometry-based technique called isotopic ratio outlier analysis (IROA). In an IROA protocol, control and experimental samples are isotopically labeled with 95 and 5%  $^{13}\text{C}$ , and the two sample populations are mixed together for uniform extraction, sample preparation, and LC-MS analysis. This labeling strategy provides several advantages over conventional approaches: (1) compounds arising from biosynthesis are easily distinguished from artifacts, (2) errors from sample extraction and preparation are minimized because the control and experiment are combined into a single sample, (3) measurement of both the molecular weight and the exact number of carbon atoms in each molecule provides extremely accurate molecular formulas, and (4) relative concentrations of all metabolites are easily determined. A heat-shock perturbation was conducted on *C. elegans* to demonstrate this approach. We identified many compounds that significantly changed upon heat shock, including several from the purine metabolism pathway. The metabolic response information by IROA may be interpreted in the context of a wealth of genetic and proteomic information available for *C. elegans*. Furthermore, the IROA protocol can be applied to any organism that can be isotopically labeled, making it a powerful new tool in a global metabolomics pipeline.



Isotopic ratio outlier analysis (IROA)<sup>1</sup> is a mass-spectrometry-based technique that discriminates molecules of biological origin from nonbiological artifacts in two-group studies (Figure 1). Similar to other stable isotope labeling strategies,<sup>2–6</sup> biomolecules are randomly labeled with the stable isotope  $^{13}\text{C}$  and are mixed together for uniform extraction, sample preparation, and LC-MS quantitative analysis. However, unlike other stable isotope labeling methods, the IROA protocol utilizes a level of enrichment of 95 and 5%  $^{13}\text{C}$  for the control and experimental populations, respectively, rather than natural abundance and 98–99% enrichment. This strategy leads to more observable isotopic peaks in the mass spectra in predictable and diagnostic patterns. The isotopologue clusters that arise from the control (95%  $^{13}\text{C}$ ) and experimental (5%  $^{13}\text{C}$ ) groups are readily distinguished not only from one another but also from compounds at natural abundance, forming easily recognizable patterns that can be used to discriminate metabolites of biological origin from artifactual signals, which do not present IROA patterns and so are effectively removed from the analysis. In addition, the ratios of

the intensities from the 95%  $^{13}\text{C}$  and 5%  $^{13}\text{C}$  populations provide a means for relative quantitation of compounds. IROA also provides a simple, rapid method for determining the number of carbons in each molecule of biological origin. The number of carbons, combined with the accurate mass from high-resolution mass spectrometry, more accurately identifies molecular formulas than accurate mass alone, providing a convenient platform for global metabolomics experimentation.

The nematode *Caenorhabditis elegans* (commonly called the ‘worm’) is one of the best-studied animals in science, primarily because of the range of relatively simple experimental protocols that allow extremely detailed manipulations. Genetics are especially well developed in *C. elegans*,<sup>7</sup> which has both self-fertilizing hermaphrodites and males and thus allows great flexibility in establishing and maintaining novel genetic lines. The animals grow easily on agar plates or liquid culture with

**Received:** August 10, 2013

**Accepted:** November 25, 2013

**Published:** November 25, 2013

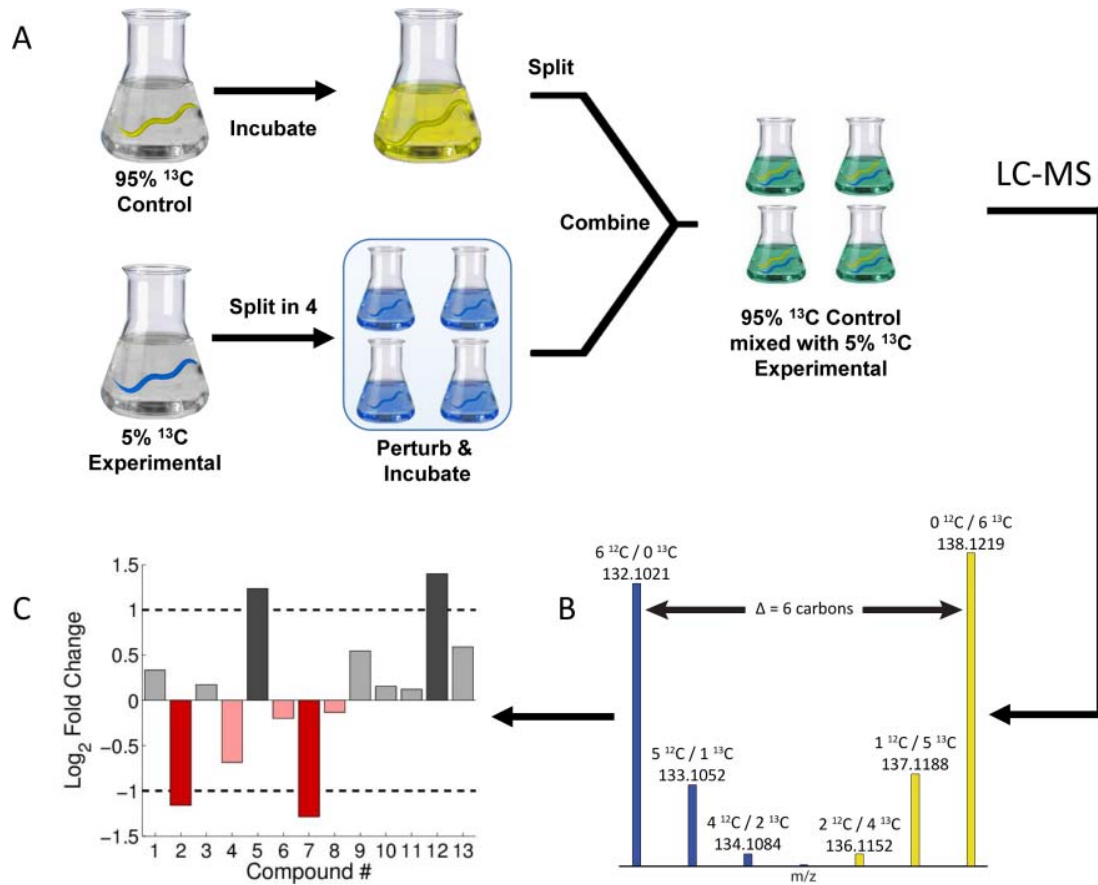


**Figure 1.** IROA Method. (A) Experimental and control groups of worms are isotopically labeled at 5 or 95%  $^{13}\text{C}$  and grown to young adult. The experimental group is split into four replicates and is perturbed, while the control group is not split. After incubation, the control group is split into four replicates, and each replicate is mixed 1:1 with an experimental replicate for uniform sample preparation and LC-MS analysis. (B) Biological compounds are easily distinguished from artifacts by the recognizable pattern caused by the isotopic enrichment. (C) Using automated software, the fold changes for all detected biological compounds can be determined. The data in C are simulated.

*Escherichia coli* as its food, and under laboratory conditions have a generation time of 3.5 days from fertilized egg to reproducing adult. It is easy to manipulate large numbers of worms that can be synchronized and grown to a defined developmental stage.<sup>8</sup>

Despite the wealth of information in genetics, cell biology, and developmental biology, metabolomic and chemical biology studies in *C. elegans* have only recently become active areas of research. Most notable has been the research on a large family of molecules called ascarosides,<sup>9,10</sup> which act as regulators of development,<sup>11,12</sup> mating attraction,<sup>8,13</sup> aggregation,<sup>14,15</sup> dispersal,<sup>16</sup> and olfaction.<sup>17</sup> Other studies have examined metabolomic differences between mutant *C. elegans*,<sup>18–20</sup> providing additional insight into genetic changes. Clearly, there are outstanding opportunities to leverage the wealth of biological information and ease of manipulation with the power of modern metabolomics approaches.

Stable isotope labeling strategies of *C. elegans* have frequently been applied to proteomic studies with  $^{15}\text{N}$  as well as some targeted  $^{13}\text{C}$  experiments, but they have only recently been applied to metabolomic studies. Recent work has utilized uniform  $^{13}\text{C}$  into *C. elegans* for improved sensitivity in NMR metabolomic studies.<sup>21</sup> Several in vivo isotopic labeling strategies have been developed to accurately identify and quantify proteins<sup>22–24</sup> and fatty acids<sup>25</sup> in *C. elegans*. Two of the most commonly used methods in proteomics include total metabolic  $^{15}\text{N}$  labeling<sup>26,27</sup> and more recently, stable-isotope

labeling with amino acids in cell culture (SILAC) mass spectrometry using either  $^{15}\text{N}$  or  $^{13}\text{C}$  labeling.<sup>23,28,29</sup> Though useful, such labeling strategies are not without limitations. Total metabolic  $^{15}\text{N}$  labeling strategies are sensitive to enrichment levels and naturally occurring isotopes such as  $^{13}\text{C}$ , making automated interpretation difficult as well as greatly affecting peptide identification and quantification.<sup>26,30</sup> SILAC mass spectrometry only labels certain amino acids (commonly Lys and Arg), which allows for accurate quantification of proteins,<sup>23,28</sup> but studies can be complicated by the conversion of isotope-labeled amino acids to other amino acids. All aforementioned strategies depend upon having fully labeled and unlabeled molecules in the respective experimental sections.

Another method, developed for fatty acid absorption and synthesis, analyzed the lysates of worms fed a 1:1 mixture of  $^{13}\text{C}$  labeled and unlabeled bacteria. The lysates were then compared via GC-MS to quantify dietary and synthesized fatty acids.<sup>25</sup> Using this method, both dietary and synthesized fatty acids are interrogated from the same worm population, eliminating any within-sample variation. A limitation of these labeling techniques is the inability to distinguish signals of biological origin from the noise (artifacts) because more than one of the isotopic peaks will usually not be detected.

Here, we demonstrate that the IROA protocol employing isotopic labeling of the two samples with 95 and 5%  $^{13}\text{C}$  circumvents many of the limitations of these other isotopic

labeling methods. It permits compounds arising from biosynthesis to be readily distinguished from artifacts and provides straightforward determination of the number of carbon atoms in each molecule to provide more accurate molecular formulas.

## EXPERIMENTAL SECTION

**Chemicals and Reagents.** Unless otherwise noted, all chemicals were purchased from Thermo Fisher Scientific, Inc. (Fairlawn, NJ). Randomly, 95 and 5%  $^{13}\text{C}$  isotopically labeled glucose were obtained from IROA Technologies (Ann Arbor, MI) as a dry powder. Magnesium sulfate heptahydrate ( $\text{MgSO}_4 \cdot 7\text{H}_2\text{O}$ ) was purchased from United States Biochemicals (Cleveland, OH). Unlabeled thiamine hydrochloride and unlabeled nystatin were purchased from Sigma-Aldrich (St. Louis, MO).

**Labeling of Bacteria.** *E. coli* MG1655 was grown in M9 minimal media on either 95 or 5%  $^{13}\text{C}$  glucose. The M9 minimal media contained 10 mg/L of unlabeled (natural abundance) thiamine and 10 mg/L of unlabeled nystatin (used as an antifungal agent). See the Supplemental Methods for more detail.

**Labeling of Worms and IROA Protocol.** To obtain sufficiently high levels of  $^{13}\text{C}$  incorporation, two successive generations of wild-type *C. elegans* (N2) were grown on IROA-labeled *E. coli* (Figure 1). The worms were grown in S-complete buffer, which contained 10 mM unlabeled potassium citrate and 5 mg/L of unlabeled cholesterol (necessary for proper worm development). See the Supplemental Methods for more detail. The worms were synchronized as previously described.<sup>8,31</sup> Upon reaching the young adult stage, the experimental population (i.e., those grown on 5%  $^{13}\text{C}$ -labeled *E. coli*) was divided into four replicates and treated with a 30 min heat shock at 33 °C in the absence of food while shaking. The control population (i.e., those grown on 95%  $^{13}\text{C}$ -labeled *E. coli*) was not split and was incubated at room temperature for the same amount of time in the absence of food. After incubation, each sample was held for an additional 1.5 h at 22 °C while shaking. The control population was then divided into four equal populations, combined 1:1 with the experimental batches, and immediately placed on ice. This mixing procedure yielded four replicate flasks that contained approximately equal quantities of both control and experimental worms. Accurate mixing is not required as the data are normalized prior to analysis.

**Metabolite Extraction.** Each flask was separated into supernatant (exometabolome) and worm pellet (endometabolome) by centrifugation. The supernatant was filtered and lyophilized, whereas the worm pellets were homogenized using a Biospec Mini-Beadbeater-8 in 80% methanol<sup>32</sup> and subsequently dried. Both samples were lyophilized and resuspended in 100 µL of LC-MS grade H<sub>2</sub>O.

**Liquid Chromatography–Mass Spectrometry.** Samples were analyzed using a mass range of  $m/z$  70–800 in positive and negative ionization mode, externally calibrated, using a Thermo Scientific Q-Exactive Orbitrap mass spectrometer equipped with an Open Accela autosampler and an Accela 1250 pump (San Jose, CA). The Q-Exactive was equipped with a heated electrospray ionization (HESI) source, which operated at a spray temperature of 500 °C, a spray voltage of 3 kV, and sheath and auxiliary gas flow rates of 60 and 10 arbitrary units, respectively. Three microliters of each sample were injected onto a Thermo Scientific Gold aQ (150 × 2.1 mm, 1.9 µm) column using a column temperature of 40 °C and a flow rate of

600 µL/min with a gradient of solvent A (0.1% formic acid in water) and solvent B (0.1% formic acid in acetonitrile) from 100% solvent A for 1 min followed by a linear gradient to 20% B in 6 min, a linear gradient to 60% B in 2 min, a linear gradient to 95% B in 4 min, held for 2 min, and a 3.5 min return to the starting composition. The inlet to the Orbitrap was held at a temperature of 320 °C, and the S-lens RF Level was set to 35%. The FR resolution was set to 70 000 at  $m/z$  200. The accuracy achieved was routinely less than 1.5 ppm, externally calibrated.

**LC-MS/MS.** LC-MS/MS analysis using data-dependent scanning was performed on a Thermo Scientific LTQ Velos mass spectrometer to aid in the identification of IROA peaks (Figure S-1). The instrument was equipped with an Accela 600 HPLC pump. Samples (3 µL in volume) were injected onto an ACE Excel 2 µm PFP column (100 × 2.1 mm). The chromatographic run utilized the same aforementioned solvent system with a gradient beginning at 1% solvent B (held for 1 min), followed by a linear ramp to 40% solvent B over 9 min, followed by an isocratic period of 2 min, followed by a linear ramp to 60% B over 1 min, followed by a 1 min isocratic period, and a 30 s ramp to starting conditions. The column was then allowed to re-equilibrate for 5.5 min prior to the following injection, amounting to a total acquisition time of 20 min. Similar to the Orbitrap, the Velos was equipped with a HESI source. The HESI source was operated with a heater temperature of 300 °C, a spray voltage of 3 kV, and sheath and auxiliary gas flows of 40 and 10 arbitrary units, respectively. The inlet temperature for the heated capillary was maintained at 350 °C, and the S-lens RF level was set to 30%. Data-dependent scanning was conducted with a normalized collision energy of 35% and an isolation width of 2 u. For these experiments, four scan events were utilized, with the first being MS, and the remaining three being MS/MS scans fragmenting the three most intense ions in scan event 1. Ions were excluded from MS/MS for a duration of 60 s following the third occurrence. It should be noted that using this protocol, MS/MS data can be collected for both the unlabeled  $^{12}\text{C}$  and fully labeled  $^{13}\text{C}$  isotopologues. In addition to data-dependent scanning, wide-isolation MS/MS experiments were conducted on targeted IROA peaks (e.g., metabolites related to the purine pathway). These experiments were conducted with an isolation width 4 u wider than the difference in mass between the  $^{12}\text{C}$  and  $^{13}\text{C}$  isotopologues, allowing for accurate determination of carbon number for fragment ions. Finally, to obtain accurate mass fragments for confirmation of specific metabolites, targeted MS/MS experiments fragmenting the  $^{12}\text{C}$  isotopologue were performed on a Thermo Scientific Q Exactive Orbitrap mass spectrometer (Figures S-6–S-16). An isolation width of 1.2 u and normalized collision energy of 35% were utilized. The same chromatographic conditions as on the Velos were used. MS/MS spectra were acquired at a spectral resolution of 17 500 on the Orbitrap. When applicable, spectra were checked against the METLIN Metabolite and Tandem MS/MS Database or the Human Metabolome Database for confirmation.

**IROA Peak Finding.** IROA peaks were identified in the raw spectral data using custom software written in-house using MATLAB. Software details are described in the Supplemental Methods. A new version of the IROA peak finder software developed by IROA Technologies will be used in future experiments and is available through IROA Technologies.

**Feature Identification.** Features were identified on the basis of both molecular formula and tandem mass spectrometry

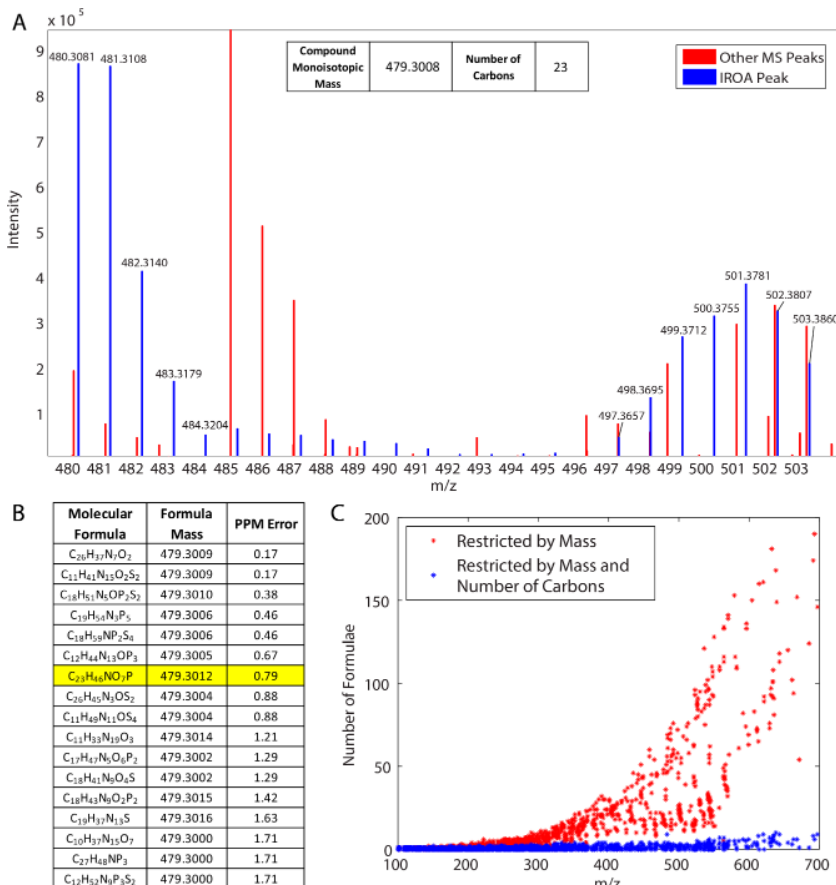


**Figure 2.** IROA allows for the discrimination between biological molecules and artifacts and constrains the number of possible molecular formulas. (A) Representative mass spectrum from a single scan in the IROA experiment. Blue peaks indicate isotope peaks originating from a single biological compound, tentatively identified as the  $[M + H]^+$  of lysophosphatidylethanolamine 18:1. An  $[M + Na]^+$  peak was also observed helping to confirm the protonated form. The fold change of this compound can be quantified by determining the ratio between the sum of the intensities of the unlabeled  $^{12}\text{C}$  peak (480.3081) and its associated isotopic peaks (481.3108, 482.3140, etc.) to the sum of the intensities of the fully labeled  $^{13}\text{C}$  base peak (503.3860) and its associated isotopic peaks (502.3807, 501.3781, etc.). (B) A table detailing the possible molecular formulas for the monoisotopic mass of this compound. Of the 17 possible molecular formulas within 2 ppm mass error for the compound in (A), only one has the correct number of carbons,  $\text{C}_{23}\text{H}_{46}\text{NO}_7\text{P}$  (highlighted). (C) The number of possible molecular formulas for a compound is greatly restricted when the exact number of carbons is used as a constraint. The possible molecular formulas within 2 ppm for 3131 IROA peaks were generated with (blue) or without (red) constraining for the number of carbons. For both (B) and (C), the formulas were generated using HR2, allowing the elements C, H, N, O, P, and S and a mass error of up to 2 ppm. Formulas were filtered using the seven golden rules with the exception of the isotopic pattern filter.<sup>46</sup>

(MS/MS) (Figures S-1, S-6–S-16) whenever possible. Because authentic standards were not available for this experiment, formulas associated with more than one isobaric compound were tentatively named by the compound with the lowest KEGG ID. In cases where isobaric compounds elute at multiple retention times, the compound with the highest total ion intensity was used for analysis (as in Figure 3A,B). Molecular formulas were generated using HR2, allowing the elements C, H, N, O, P, and S and a mass error of up to 2 ppm. Formulas were filtered using the seven golden rules with the exception of the isotopic pattern filter.<sup>33</sup> Formulas with the incorrect number of carbons were discarded.

**Data Analysis and Statistics.** Significant fold changes were evaluated for the endometabolome and exometabolome separately using only those metabolites that were detected in at least three out of four replicates. False discovery rate (FDR) corrections were used for multiple testing across metabolites, using a resampling-based FDR controlling approach. Significance was determined by having an average absolute log fold

change of 0.585 ( $\log_2 1.5$ ) and passing a *t* test with a FDR of 0.05.<sup>34</sup>

## RESULTS

A primary requirement in an IROA experiment is the total isotopic labeling of samples. *C. elegans* is an ideal animal to demonstrate the utility of IROA studies because it feeds on bacteria, which may be isotopically labeled by growth in minimal media supplemented with  $^{13}\text{C}$ -labeled glucose. Randomly labeling worms with 5 or 95%  $^{13}\text{C}$  enriches the  $^{13}\text{C}$  content in all biogenic compounds, thereby facilitating detection of multiple  $^{13}\text{C}$  isotopic peaks. In conventional analyses with natural abundance (1.1%  $^{13}\text{C}$ ) low molecular weight compounds, more than one isotopic peak is usually not detectable or simply treated as noise. To illustrate the utility of IROA for global metabolomics, we exposed wild-type (N2) worms to a heat shock (Figure 1), which causes significant, widespread changes in metabolism.<sup>30</sup> We collected and analyzed material from the exometabolome (all material that

worms release in the supernatant) and the endometabolome (homogenized total extracts from the worm bodies). We used a 30 min heat shock at 33 °C because these conditions were sufficient to activate the stress reporter *daf-16* without causing significant mortality (data not shown).<sup>35</sup> This protein is a transcription factor known to be involved in aging and stress resistance and is activated upon heat shock, whereby it translocates to the nucleus and activates other proteins involved in the heat-shock response.

#### Distinguishing Biological Compounds from Noise.

The differentiation of peaks originating from biogenic compounds versus noise is a challenge in untargeted mass spectrometric studies. Using IROA, the increased abundance of <sup>13</sup>C in biogenic compounds leads to predictable isotope patterns that can be used to distinguish biogenic peaks from artifactual noise. This is demonstrated in Figure 2A with an expansion of an IROA peak of the [M + H]<sup>+</sup> of the lysophosphatidylethanolamine (LPE) 18:1. The blue peaks are the isotopologues ranging from the monoisotopic <sup>12</sup>C peak on the left to the fully incorporated <sup>13</sup>C peak on the right. These peaks can be distinguished from peaks from other compounds or background noise (red) in the scan based on two criteria: mass spectral peak spacing (the mass difference between <sup>12</sup>C and <sup>13</sup>C is 1.0034 u) and relative intensity. The relative intensities of an IROA peak follow a binomial distribution, which is dependent on the percent incorporation of <sup>13</sup>C and the number of carbons in the compound. The number of carbons in this compound is determined by recognizing that the mass difference between the <sup>12</sup>C monoisotopic and the <sup>13</sup>C monoisotopic peaks indicates 23 carbons. This combination of peak spacing and the shape of the associated peaks not only serves to ensure that all selected peaks are correctly assigned but also will be so statistically rare that noise is effectively excluded.

**Accurate Molecular Formula Determination.** With the constraints described in the methods, there were 17 possible molecular formulas predicted for the *m/z* of 480.3081 without constraining for carbon number (Figure 2B). This protonated species was determined by the presence of the sodiated ion being present at the same retention time. When combining accurate mass with definitive knowledge of carbon number, the number of formulas reduces to one possibility. We should note that several other strategies exist for constraining molecular formulas; however, they either also require isotopic labeling<sup>36,37</sup> or require an instrument capable of high accuracy with respect to ion intensities.<sup>33</sup> Using this technique, as the detection limits of the labeled metabolites are reached, the relative spectral errors will exceed the limits of the assay.<sup>38</sup>

Similar to the above exercise, an accurate knowledge of the number of carbons for most compounds restricts the possible number of molecular formulas for a given mass, as shown in Figure 2C. In this example, molecular formulas were generated for each IROA peak in one replicate sample from the endometabolome. For each experimental IROA peak, the number of possible formulas with less than 2 ppm error generated using the accurate mass was plotted as a circle in red, while the number of possible formulas after removing formulas with the incorrect number of carbons was plotted as a circle in blue. This further demonstrates that knowledge of the number of carbons reduces the possible number of molecular formulas for an unknown compared to mass accuracy of the <sup>12</sup>C peak alone.

**Detection of Thousands of Metabolites.** In a typical high-resolution LC-MS experiment, there may be millions of individual mass spectral peaks detected, very few of which originate from biogenic molecules. Table 1 summarizes the

**Table 1. Data Reduction and Analysis of IROA Peaks**

ionization mode	endometabolome			exometabolome		
	pos	neg	total	pos	neg	total
IROA peaks in any sample <sup>a</sup>	4883	3825	8708	1533	1262	2795
IROA peaks in ≥3 replicates <sup>b</sup>	1613	1302	2915	527	532	1059
In ≥ 3 replicates, with at least one match in HMDB <sup>c</sup>	565	388	953	250	237	487
In ≥ 3 replicates, significantly changed <sup>d</sup>	300	205	505	191	159	350
In ≥ 3 replicates, significantly changed, match HMDB <sup>e</sup>	69	54	123	107	78	185

<sup>a</sup>Unique IROA peaks that appear in at least one replicate. For example, if an IROA peak with a mass of 123.1234 and elution time of 120 s is detected in two replicates, it is counted once. <sup>b</sup>Unique IROA peaks that appear in at least three out of four replicates within either the pellet or the supernatant. <sup>c</sup>Match by mass within ±0.002 u and have the correct number of carbons. <sup>d</sup>Significance was determined by having an average absolute log fold change of 0.585 ( $\log_2 1.5$ ) and passing a *t* test with a FDR of 0.05. <sup>e</sup>Of the significant IROA peaks, the number which had at least one match in HMDB.

numbers of IROA peaks found in this study after heat-shock perturbation, with analysis of both the endometabolome (endo) and exometabolome (exo) of the worms in both positive and negative mode. In at least one replicate in either ionization mode, 8708 (endo) and 2795 (exo) unique IROA peaks were found. These IROA peaks present a significant reduction as compared to the millions of mass spectral peaks from an average unaligned chromatographic run. Of the detected IROA peaks, 2915 (endo) and 1059 (exo) were found in at least three out of four replicates. Of those, 953 (endo) and 487 (exo) yielded matches of at least one compound in the HMDB database.<sup>39</sup> Furthermore, out of the IROA peaks present in ≥3 replicates, 505 (endo) and 350 (exo) were significantly affected by the heat shock perturbation. We are in the process of confirming many of these annotations by MS<sup>n</sup> (See the Supplementary Files; these data are available as an Excel file).

**Purines Are Highly Affected by Heat Shock.** In this experiment, we were able to measure the changes in the concentrations of 21 compounds in the human purine metabolism pathway (KEGG: ko00230) in heat-shocked worms (Figure 3). Figure 3A shows the  $\log_2$  fold changes for these compounds in the endometabolome (purple) and exometabolome (gold). A reconstructed KEGG pathway map (Figure 3B) projects our experimental IROA data onto the KEGG purine pathway, and each node is colored by the fold change in the endometabolome. Several compounds such as guanine, hypoxanthine, and uric acid are downregulated in the endometabolome, while others such as GMP, hypoxanthine, and inosine are upregulated in the exometabolome (Figure 3C).

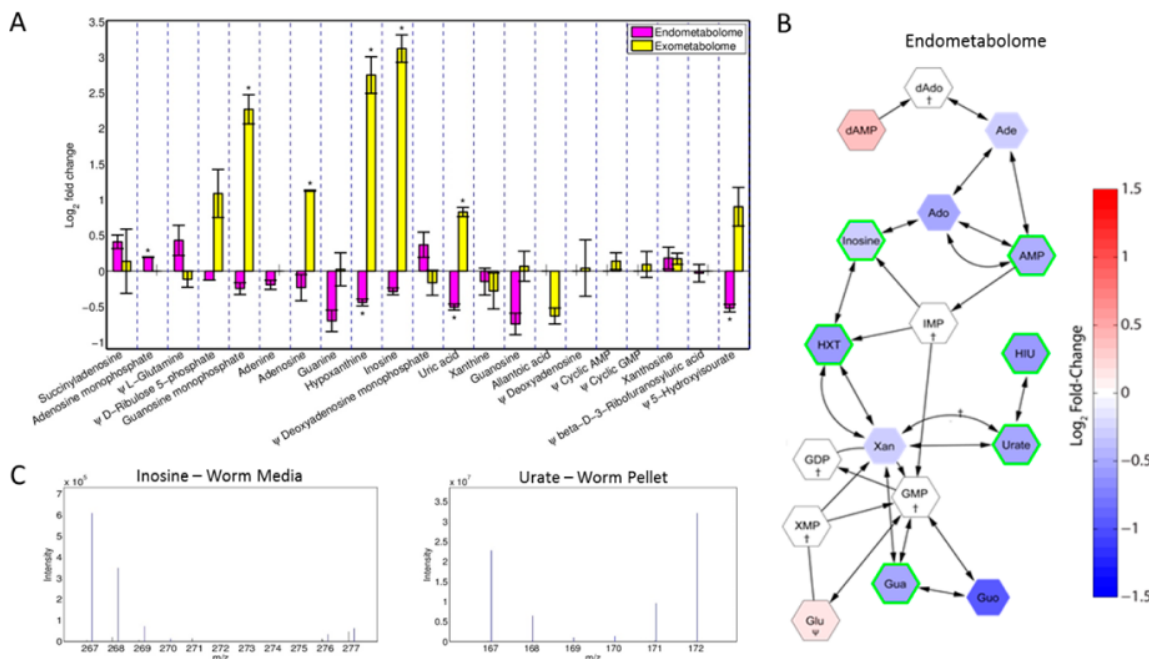


**Figure 3.** IROA allows for the relative determination of changes in metabolites. (A) The fold changes for 21 compounds in the KEGG Purine Metabolism pathway are shown for the endo- and exometabolomes. Values represent means ( $n \geq 3$ ), and the error bars are the standard deviation. A bar without upper or lower bounds (l) indicates that the compound was detected in less than three replicates and is therefore not included in the analysis. Bars with one asterisk (\*) indicate significant changes ( $P < 0.001$ ). (B) A section of the human purine metabolism pathway from KEGG is shown as a network with metabolites as nodes and reactions as edges. Compounds included in this network were either detected in this experiment or are annotated as participating in a reaction with a detected compound. The nodes are colored according to the  $\log_2$  fold changes in the pellets of heat-shocked worms. Nodes marked with a dagger ( $\dagger$ ) were not found in this experiment. Nodes with a green border indicate that the fold changes were significant ( $P < 0.001$ ). All compounds, except those marked with a Psi ( $\Psi$ ), were confirmed by MS-MS (Figures S-6–S-16). Nonstandard abbreviations: dAdo, deoxyadenosine; Ade, adenine; Ado, adenosine; HXT, hypoxanthine; HIU, 5-hydroxysourate; Xan, xanthine; XMP, xanthosine 5'-phosphate; Gua, guanine; Guo, guanosine. (C) An IROA peak for the  $[M - H]^-$  of inosine demonstrates an increase of the 5%  $^{13}\text{C}$  labeled sample relative to the 95%  $^{13}\text{C}$  labeled sample indicating an increase in inosine in the released exometabolome of heat-shocked worms relative to the control (left). An IROA peak for urate demonstrates a relative decrease in urate in the endometabolomes of heat-shocked worms (right).

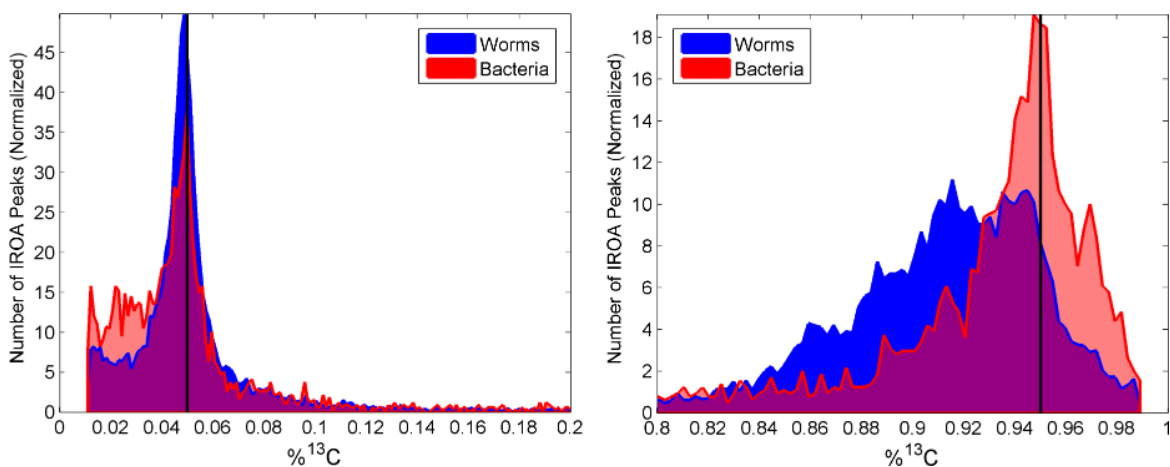


**Figure 4.** Distribution of isotopic labels in IROA experiments. Histograms indicate the actual percent  $^{13}\text{C}$  incorporation for each IROA peak for the labeling of worms (blue) and bacteria (red) with 5%  $^{13}\text{C}$  glucose (left) and 95%  $^{13}\text{C}$  glucose (right). Black lines are drawn at 5% (left) and 95% (right).

## DISCUSSION

The IROA experiment presented here provides a high quality and detailed snapshot of the *C. elegans* metabolome under stress. IROA labeling allowed for a significant and automated data reduction to several thousand features (Table 1) that were biosynthesized by either the worms or their bacterial feedstock.

However, because the worms were subjected to sucrose floatation before the heat-shock challenge, which removes the bacteria, metabolites recorded in the IROA experiments were isolated from the worms. The IROA protocol allowed for an automatic measurement of fold changes for all metabolites under heat-shock stress. Since a common control was combined internally to each experimental sample, against

which the response was measured, it would be subjected to identical sample preparation losses. Furthermore, using IROA the pooled samples will be analyzed under identical conditions and thus will have very small sample-to-sample variance and ion suppression differences between the experimental and control samples, similar to SILAC, iTRAQ, and other pooled sample protocols.

In this experiment, not all IROA peaks conformed to their expected peak shapes. The source of this peak shape deviation was usually in the direction of a  $^{13}\text{C}$  isotope dilution; rather than the expected 95%  $^{13}\text{C}$  incorporation, some compounds were found at 92% or even lower (Figure 4). This variation from the expected percentage was easily accommodated in software as the peak was still identified as an IROA peak (by their mass spacing and intensities), and the respective monoisotopic peaks could be identified. Possible sources of contaminating  $^{12}\text{C}$  include: citrate used in the worm growth media, natural abundance cholesterol (which is required for proper worm development), incorporation of  $\text{CO}_2$  from the environment, and incomplete and/or differential labeling of metabolites in the bacterial food source.<sup>5</sup> As shown in Figure 4, the IROA peaks found in the bacterial food source also show differential labeling (i.e., they are not all exactly 5 and 95%  $^{13}\text{C}$ ). The bacterial  $^{13}\text{C}$  dilution is almost certainly from the S-complete buffer, which contains unlabeled citrate. Bacteria are grown in M9 minimal media and then transferred to the S-complete buffer for coculturing with worms, where they can briefly incorporate unlabeled citrate before they are frozen for inactivation before feeding to worms. We are investigating noncarbon buffer alternatives to this standard *C. elegans* culture medium. It is likely that the contaminating  $^{12}\text{C}$  can lead to incorporation differences in specific pathways (Figure S-2), but a full analysis is beyond the scope of this paper.

We wanted to rule out the possibility of incomplete labeling of our starting material ( $^{13}\text{C}$  glucose). Using NMR, we quantified the relative amount of impurities in the 5  $^{13}\text{C}$  and 95%  $^{13}\text{C}$  glucose and found an approximately 0.5% w/w impurity of natural abundance  $^{13}\text{C}$  acetate (Figure S-3). We also measured the percent  $^{13}\text{C}$  labeling at 5.3% and 95.5% by mass spectrometry (Figures S-4, S-5). We conclude that the starting material was sufficiently pure and not the source of the  $^{13}\text{C}$  dilution.

The  $^{13}\text{C}$  dilution raises the possibility of isotope effects caused by the unequal labeling of metabolites leading to miscalculations in fold changes.<sup>40</sup> Future experiments will use an augmented reference design consisting of a reference population of 95%  $^{13}\text{C}$  worms to decouple isotope effects from biological changes. Perturbation will be employed on 5%  $^{13}\text{C}$  labeled experimental worms and compared to 5%  $^{13}\text{C}$  labeled control worms, using the 95%  $^{13}\text{C}$  worms as a “reference” population. By decoupling the experimental variation from the isotopic variation, we will be able to more accurately quantify fold changes of metabolites regardless of biases in labeling.

One of the obvious challenges is the difficulty in unambiguously naming peaks without authentic standards. This problem is common to all mass spectrometric metabolomics approaches and is not unique to IROA. The number of unambiguously named compounds could be further increased with an extensive library of standards, a database of retention times, or by using physical properties of potential compounds to estimate retention times and model chromatographic data.<sup>41</sup> The number of named IROA peaks could be

increased by expanding our database searching beyond HMDB, which does not include nematode-specific compounds, and by improving the IROA software to match adducts and fragments with their base peak. For IROA peaks that are not in databases or standard libraries, it should be straightforward to incorporate NMR or MS/MS analysis on the isolated peak, even if it is a mixture.<sup>42</sup>

We observed consistent decreases in the concentrations of several compounds in the KEGG purine pathway in the endometabolome of heat-shocked worms. These results suggest the involvement of purines in stressed worms, possibly as a result of an overall slowdown of transcription. Guanine, guanosine, hypoxanthine, and uric acid, four of the most highly down-regulated compounds, are involved in the salvage and biosynthesis of purines. The increase in several purines seen in the exometabolome such as adenosine, inosine, and hypoxanthine may be a result of death and potentially lysis of heat-shocked worms leading to release and degradation of purine compounds such as ADP and ATP. A more in-depth analysis will be reserved for future experiments.

While the primary goal of this study was to demonstrate the IROA technique, the results of this experiment will direct our future experiments to better understand worm communication and interaction with their environment. *C. elegans* possesses many evolutionarily conserved pathways involved in stress and innate immunity,<sup>43</sup> the study of which can lead to improved understanding of these networks in higher organisms.<sup>44,45</sup>

## CONCLUSIONS

The IROA protocol provides outstanding coverage of the global metabolome by (1) allowing for simple discrimination between biosynthesized molecules and artifacts, (2) reducing error associated with sample preparation and extraction by combining the experiment and control, (3) providing both the molecular weight and the number of carbon atoms in each metabolite to obtain much more accurate molecular formulas, and (4) enabling the automated measurement of relative concentrations of metabolites under different conditions. This protocol should become an outstanding new tool to provide detailed metabolic information in the large numbers of characterized *C. elegans* genetic strains and in any organism or cell culture that can be isotopically labeled. The data from this study will be deposited with the Metabolomics Workbench Metabolite Database (<http://www.metabolomicsworkbench.org/>) at the University of California, San Diego, as recommended by the NIH Metabolomics Common Fund.

## ASSOCIATED CONTENT

### Supporting Information

This material is available free of charge via the Internet at <http://pubs.acs.org>.

## AUTHOR INFORMATION

### Corresponding Author

\*E-mail: aedison@ufl.edu.

### Author Contributions

C.B. developed IROA; G.S.S., C.S.C., and R.A. designed, planned, and executed the worm labeling and sample preparation; M.S. collected the LC-MS data; G.S.S. and C.B. analyzed the LC-MS data; R.F.M. and T.G. collected and analyzed the MS/MS data; R.A.Y. and R.F.M. assisted with data interpretation; A.S.E. and C.B. designed the experiment; A.S.E.,

G.S.S., and C.S.C. wrote the paper with significant contributions from all authors.

### Author Contributions

• These authors contributed equally to this study.

### Notes

The authors declare the following competing financial interest(s): C.B. is the inventor of IROA, which is patented and licensed to IROA Technologies.

### ACKNOWLEDGMENTS

NIH provided funding for this study (5R01GM085285-04 to ASE), some of which was done in the Southeast Center for Integrated Metabolomics (NIH U24 DK097209-01A1). Caroline Williams, Daniel Hahn, and Lauren McIntyre provided very helpful suggestions throughout this project. Profs. Paul Sternberg, Frank Schroeder, and Burt Singer provided many helpful discussions about *C. elegans*. We thank Prof. Jeannine Brady for the use of her Mini-Beadbeater. Prof. Paul Gulig provided the *E. coli* strain MG1655.

### REFERENCES

- (1) de Jong, F. A.; Beecher, C. *Bioanalysis* **2012**, *4*, 2303–2314.
- (2) Lu, W.; Kwon, Y. K.; Rabinowitz, J. D. *J. Am. Soc. Mass Spectrom.* **2007**, *18*, 898–909.
- (3) Mashego, M. R.; Wu, L.; Van Dam, J. C.; Ras, C.; Vinke, J. L.; Van Winden, W. A.; Van Gulik, W. M.; Heijnen, J. *J. Biotechnol. Bioeng.* **2004**, *85*, 620–628.
- (4) Wu, L.; Mashego, M. R.; van Dam, J. C.; Proell, A. M.; Vinke, J. L.; Ras, C.; van Winden, W. A.; van Gulik, W. M.; Heijnen, J. *J. Anal. Biochem.* **2005**, *336*, 164–171.
- (5) Bennett, B. D.; Yuan, J.; Kimball, E. H.; Rabinowitz, J. D. *Nat. Protoc.* **2008**, *3*, 1299–1311.
- (6) Birkemeyer, C.; Luedemann, A.; Wagner, C.; Erban, A.; Kopka, J. *Trends Biotechnol.* **2005**, *23*, 28–33.
- (7) Brenner, S. *Genetics* **1974**, *77*, 71–94.
- (8) Srinivasan, J.; Kaplan, F.; Ajredini, R.; Zachariah, C.; Alborn, H. T.; Teal, P. E.; Malik, R. U.; Edison, A. S.; Sternberg, P. W.; CC, S. F. *Nature* **2008**, *454*, 1115–1118.
- (9) Edison, A. S. *Curr. Opin. Neurobiol.* **2009**, *19*, 378–388.
- (10) Ludewig, A. H.; Schroeder, F. C. *WormBook* **2013**, 1–22.
- (11) Jeong, P. Y.; Jung, M.; Yim, Y. H.; Kim, H.; Park, M.; Hong, E.; Lee, W.; Kim, Y. H.; Kim, K.; Paik, Y. K. *Nature* **2005**, *433*, 541–545.
- (12) Butcher, R. A.; Fujita, M.; CC, S. F.; Clardy, J. *Nat. Chem. Biol.* **2007**, *3*, 420–422.
- (13) Pungaliya, C.; Srinivasan, J.; Fox, B. W.; Malik, R. U.; Ludewig, A. H.; Sternberg, P. W.; CC, S. F. *Proc. Natl. Acad. Sci. U.S.A.* **2009**, *106*, 7708–7713.
- (14) Macosko, E. Z.; Pokala, N.; Feinberg, E. H.; Chalasani, S. H.; Butcher, R. A.; Clardy, J.; Bargmann, C. I. *Nature* **2009**, *458*, 1171–1175.
- (15) Srinivasan, J.; von Reuss, S. H.; Bose, N.; Zaslaver, A.; Mahanti, P.; Ho, M. C.; O'Doherty, O. G.; Edison, A. S.; Sternberg, P. W.; CC, S. F. *PLoS Biol.* **2012**, *10*, e1001237.
- (16) Kaplan, F.; Alborn, H. T.; von Reuss, S. H.; Ajredini, R.; Ali, J. G.; Akyazi, F.; Stelinski, L. L.; Edison, A. S.; Schroeder, F. C.; Teal, P. E. *PLoS One* **2012**, *7*, e38735.
- (17) Yamada, K.; Hirotsu, T.; Matsuki, M.; Butcher, R. A.; Tomioka, M.; Ishihara, T.; Clardy, J.; Kunitomo, H.; Iino, Y. *Science* **2010**, *329*, 1647–1650.
- (18) Castro, C.; Krumsiek, J.; Lehrbach, N. J.; Murfitt, S. A.; Miska, E. A.; Griffin, J. L. *Mol. Biosyst.* **2013**, *9*, 1632–1642.
- (19) Martin, F.-P. J.; Spanier, B.; Collino, S.; Montoliu, I.; Kolmeder, C.; Giesbertz, P.; Affolter, M.; Kussmann, M.; Daniel, H.; Kochhar, S.; Rezzi, S. *J. Proteome Res.* **2011**, *10*, 990–1003.
- (20) Blaise, B. J.; Giacomotto, J.; Elena, B.; Dumas, M. E.; Toulhoat, P.; Segalat, L.; Emsley, L. *Proc. Natl. Acad. Sci. U.S.A.* **2007**, *104*, 19808–19812.
- (21) An, Y. J.; Xu, W. J.; Jin, X.; Wen, H.; Kim, H.; Lee, J.; Park, S. *ACS Chem. Biol.* **2012**, *7*, 2012–2018.
- (22) Tops, B. B.; Gauci, S.; Heck, A. J.; Krijgsveld, J. *J. Proteome Res.* **2010**, *9*, 341–351.
- (23) Larance, M.; Baily, A. P.; Pourkarimi, E.; Hay, R. T.; Buchanan, G.; Coulthurst, S.; Xiropoulos, D. P.; Gartner, A.; Lamond, A. I. *Nat. Methods* **2011**, *8*, 849–851.
- (24) Gouw, J. W.; Krijgsveld, J.; Heck, A. J. *Mol. Cell. Proteomics* **2010**, *9*, 11–24.
- (25) Perez, C. L.; Van Gilst, M. R. *Cell Metab.* **2008**, *8*, 266–274.
- (26) Gouw, J. W.; Tops, B. B.; Mortensen, P.; Heck, A. J.; Krijgsveld, J. *Anal. Chem.* **2008**, *80*, 7796–7803.
- (27) Schrimpf, S. P.; Hengartner, M. O. *J. Proteomics* **2010**, *73*, 2186–2197.
- (28) Gruhler, S.; Kratchmarova, I. *Methods Mol. Biol.* **2008**, *424*, 101–111.
- (29) Mann, M. *Nat. Rev. Mol. Cell Biol.* **2006**, *7*, 952–958.
- (30) Richter, K.; Haslbeck, M.; Buchner, J. *Mol. Cell* **2010**, *40*, 253–266.
- (31) Kaplan, F.; Srinivasan, J.; Mahanti, P.; Ajredini, R.; Durak, O.; Nimalendran, R.; Sternberg, P. W.; Teal, P. E.; CC, S. F.; Edison, A. S.; Alborn, H. T. *PLoS One* **2011**, *6*, e17804.
- (32) Geier, F. M.; Want, E. J.; Leroi, A. M.; Bundy, J. G. *Anal. Chem.* **2011**, *83*, 3730–3736.
- (33) Kind, T.; Fiehn, O. *BMC Bioinf.* **2006**, *7*, 234.
- (34) Benjamini, Y.; Yekutieli, D. *Ann. Stat.* **2001**, *29*, 1165–1188.
- (35) Henderson, S. T.; Johnson, T. E. *Curr. Biol.* **2001**, *11*, 1975–1980.
- (36) Hegeman, A. D.; Schulte, C. F.; Cui, Q.; Lewis, I. A.; Huttlin, E. L.; Eggbalnia, H.; Harms, A. C.; Ulrich, E. L.; Markley, J. L.; Sussman, M. R. *Anal. Chem.* **2007**, *79*, 6912–6921.
- (37) Giavalisco, P.; Hummel, J.; Liseic, J.; Inostroza, A. C.; Catchpole, G.; Willmitzer, L. *Anal. Chem.* **2008**, *80*, 9417–9425.
- (38) Erve, J. C. L.; Gu, M.; Wang, Y.; DeMaio, W.; Talaat, R. E. *J. Am. Soc. Mass Spectrom.* **2009**, *20*, 2058–2069.
- (39) Wishart, D. S.; Jewison, T.; Guo, A. C.; Wilson, M.; Knox, C.; Liu, Y.; Djoumbou, Y.; Mandal, R.; Aziat, F.; Dong, E.; Bouatra, S.; Sinelnikov, I.; Arndt, D.; Xia, J.; Liu, P.; Yallou, F.; Bjorndahl, T.; Perez-Pineiro, R.; Eisner, R.; Allen, F.; Neveu, V.; Greiner, R.; Scalbert, A. *Nucleic Acids Res.* **2013**, *41*, D801–D807.
- (40) Wasylenko, T. M.; Stephanopoulos, G. *Biotechnol. J.* **2013**, *8*, 1080–1089.
- (41) Creek, D. J.; Jankevics, A.; Breitling, R.; Watson, D. G.; Barrett, M. P.; Burgess, K. E. V. *Anal. Chem.* **2011**, *83*, 8703–8710.
- (42) Robinette, S. L.; Bruschweiler, R.; Schroder, F. C.; Edison, A. S. *Acc. Chem. Res.* **2012**, *45*, 288–297.
- (43) Morley, J. F.; Morimoto, R. I. *Mol. Biol. Cell* **2004**, *15*, 657–664.
- (44) Fiehn, O. *Comp. Funct. Genom.* **2001**, *2*, 155–168.
- (45) Hirai, M. Y.; Yano, M.; Goodenow, D. B.; Kanaya, S.; Kimura, T.; Awazuhara, M.; Arita, M.; Fujiwara, T.; Saito, K. *Proc. Natl. Acad. Sci. U.S.A.* **2004**, *101*, 10205–10210.
- (46) Kind, T.; Fiehn, O. *BMC Bioinf.* **2007**, *8*, 105.

